Solution Structure of a CCHHC Domain of Neural Zinc Finger Factor-1 and Its Implications for DNA Binding†

Holly J. Berkovits-Cymet,‡ Barbara T. Amann, and Jeremy M. Berg*,§

Department of Biophysics and Biophysical Chemistry, Johns Hopkins University School of Medicine, Baltimore, Maryland 21205

Received July 7, 2003; Revised Manuscript Received November 6, 2003

ABSTRACT: The structure of a CCHHC zinc-binding domain from neural zinc finger factor-1 (NZF-1) has been determined in solution though the use of NMR methods. This domain is a member of a family of domains that have the Cys-X_4-Cys-X_4-His-X_7-His-X_5-Cys consensus sequence. The structure determination reveals a novel fold based around a zinc(II) ion coordinated to three Cys residues and the second of the two conserved His residues. The other His residue is stacked between the metal-coordinated His residue and a relatively conserved aromatic residue. Analysis of His to Gln sequence variants reveals that both His residues are required for the formation of a well-defined structure, but neither is required for high-affinity metal binding at a tetrahedral site. The structure suggests that a two-domain protein fragment and a double-stranded DNA binding site may interact with a common two-fold axis relating the two domains and the two half-sites of the DNA-inverted repeat.

Sequence-specific DNA-binding proteins play crucial roles in controlling spatially and temporally regulated gene expression. Numerous structural classes from such proteins have been characterized, including several that include domains organized around bound zinc ions (*1*−*3*). A class of such proteins represented by neural zinc finger factor-1 (NZF-1)[1] has not been well characterized. The NZF-1 protein and the related protein MyT1 were discovered because of their ability to bind specific sequences found in the promoters of certain proteins expressed primarily in the mammalian nervous system (*4*, *5*). NZF-1 and MyT1 contain multiple sequences corresponding to a novel class of zinc-binding motifs. Additional members of this protein family have been characterized in mammals and in other organisms, including *Drosophila melanogaster*, *Anopheles gambiae*, *Caenorhabditis elegans*, and *Xenopus laevis* (*6*, *7*). These proteins have up to seven putative zinc-binding sequences, usually arranged in sets of two or more sequences. Where it has been investigated, these proteins are expressed primarily in the nervous system. The consensus derived from these sequences is **C**PTPG**C**(D/T)GXG**H**XXGX(Y/F)XX**H**RS(L/A)SG**C** where the indicated residues are present in more than 75% of the more than 20 known sequences with completely conserved residues underlined and Cys and His residues shown in bold.

The NZF-1 zinc-binding domains include five (rather than the more usual four) absolutely conserved potential metal ligands arranged in the Cys-X_4-Cys-X_4-His-X_7-His-X_5-Cys pattern. Because of this set of conserved residues, these domains have been termed CCHHC domains (*8*, *9*). The nature of the potential metal-binding residues and their spacing are sufficiently different from those from other classes of zinc-binding domains that it suggests that these domains fold into a distinct structure. Previous studies of peptides with one or two tandem CCHHC domains from NZF-1 have demonstrated that these domains coordinate metal ions in a tetrahedral fashion through three cysteinates and one histidine, based on the absorption spectra of the complexes formed with cobalt(II) (*8*, *9*). This observation led to two questions. Which of the two conserved histidine residues coordinates the metal ion, and what is the role of the other conserved histidine residue?

Both NZF-1 and MyT1 were identified because of their ability to bind specific double-stranded DNA sequences. Binding studies with mutated versions of natural sites and methylation interference studies have demonstrated that the core binding sequence approximates 5′-AAAGTTT-3′ (*5*, *7*) for each protein. Studies with protein fragments have demonstrated that a set of two tandem domains is sufficient for high-affinity DNA binding and that different sets of domains bind to similar sequences. Furthermore, experiments with NZF-1 have demonstrated that the protein binds in the major groove. The approximate 2-fold symmetry of the core DNA binding site (with AAA half-sites connected by a central G) and the requirement for a set of two tandem domains suggest the possibility that these proteins bind with each domain interacting with a half-site.

We report the determination of the solution structure of a fragment of NZF-1 that includes a single CCHHC domain. The structure is, indeed, distinct from any previously characterized metal-binding domain. The second of the two

† This work was supported by a grant from the National Institute of General Medical Sciences.

‡ Present address: Department of Chemistry, Merrimack College, North Andover, MA 01845.

§ Present address: National Institute of General Medical Sciences, Bethesda, MD 20892.

[1] Abbreviations: NZF-1, neural zinc finger factor-1; MyT1, myelin transcription factor-1; HPLC, high-performance liquid chromatography; HSQC, homonuclear single-quantum coherence; Tris, tris(hydroxymethyl)amine; HEPES, 4-(2-hydroxyethyl)-1-piperazineethanesulfonic acid.

10.1021/bi035159d CCC: $27.50
Published on Web 01/03/2004

conserved histidine residues within the sequence binds the zinc(II), while the first histidine plays a different role in stabilizing the structure, stacking between the metal-binding core and an aromatic residue that is relatively conserved within this domain family. The amino and carboxyl termini extend in similar directions from one end of the structure.

MATERIALS AND METHODS

Materials. A DNA fragment encoding residues 487−548 of rat NZF-1 was subcloned from a plasmid encoding residues 487−606 previously described (*8*). This fragment, hereafter called NZF-1(487−548), has the amino acid sequence MHVKKTYYDPSRTEKRESK**C**$_{20}$PTPG**C**$_{25}$-DGTG**H**$_{30}$VTGLYPH**H**$_{38}$RSLSG**C**$_{44}$PHKDRVPPEILAM-HENVLK, in which the five Cys and His residues characteristic of this class of domain are shown in bold and numbered relative to the fragment N-terminus. This fragment and a previously described fragment NZF-1(487−584) (formerly called NZF-1b) with the sequence MHVKKTYY-D P S R T E K R E S K **C** P T P G **C** D G T G **H** V T G L Y P H-**H** R S L S G **C** P H K D R V P P E I L A M H E N V L K **C** P T-PG**C**TGRG**H**VNSVRNS**H**RSLSG**C**PIAAAEKLAKA were expressed in *Escherichia coli* strain BL21(DES) pLysS and partially purified by stepwise elution with KCl from a SP-Sepharose Fast Flow column (Pharmacia). After reduction with dithiothreitol, the protein fragments were further purified on a diphenyl reversed-phase HPLC column and maintained in an anaerobic atmosphere of 3−5% hydrogen in nitrogen thereafter to minimize cysteine oxidation. NZF-1(487−548) and NZF-1(487−584) were uniformly labeled with ^{15}N using $^{15}NH_4Cl$ as the sole source of nitrogen. NZF-1(487−584) uniformly labeled with ^{15}N and ^{13}C was expressed using $^{15}NH_4Cl$ and [^{13}C]glucose as the sole sources of nitrogen and carbon, respectively (*10*). NMR samples were prepared by adding 1.0 equiv of Zn(II) or ^{113}Cd(II) per metal-binding site and adjusting the pH to 7.0 using deuterated Tris to a final buffer concentration between 36 and 55 mM. No additional salts were added. Protein fragment concentrations ranged from 1.5 to 2.8 mM.

NMR Spectroscopy and Resonance Assignments. All NMR experiments were performed on a Varian UNITY Plus 500 MHz NMR spectrometer. Homonuclear two-dimensional (2D) experiments were performed at 20 °C, and heteronuclear 2D and three-dimensional (3D) experiments were performed at 30 °C. The following spectra were recorded to obtain resonance assignments (with a TOCSY mixing time of 65 ms): ^{1}H−^{15}N HSQC (*11*), 3D ^{1}H−^{15}N HSQC-TOCSY (*11*), and ^{1}H−^{13}C HCCH-TOCSY (*12*) for NZF-1(487−584). Aromatic side chain assignments were obtained from a ^{1}H−^{13}C CT-HSQC experiment (*13*) with time delays optimized for the His ring coupling constants (J_{CC} = 70 Hz, J_{CH} = 200 Hz). The protonation states of the His rings were determined from a ^{1}H−^{15}N HSQC experiment optimized for long-range interactions between the imidazole nitrogens and the carbon-bound imidazole protons (*14*). Gradient-enhanced ^{15}N−^{13}C HNCA (*15*) and ^{15}N−^{13}C HNCACB (*16*) experiments were used for the sequential assignment of amino acid residues. The assignment of the NZF-1(487−548) peptide was assisted by the assignment of the NZF-1(487−584) peptide, but all chemical shifts were validated using ^{1}H−^{15}N HSQC (*11*) and 3D ^{1}H−^{15}N HSQC-TOCSY (*11*) data collected on the NZF-1(487−548) peptide. The 3D TOCSY and NOESY experiments were carried out with D_1−D_3 values of 512, 128, and 32 complex points, respectively. The 2D HSQC experiments were collected with 1024 and 64 complex points. Several amino acids were not assigned; notable were the seven proline residues, G24 which follows P23, R39, and S42. Other assignments not obtained included portions of the C- and N-terminal regions. NOE distance restraints were determined from homonuclear 2D NOESY (H_2O and D_2O) and 3D ^{1}H−^{15}N HSQC-NOESY (*17*) experiments collected with a mixing time of 125 ms. A ^{1}H−^{15}N HSQC experiment with ^{113}Cd-substituted NZF-1(487−548) was used for the identification of the metal-binding His residue. The FELIX 98 software package was used for data processing, and locally written programs were used for analysis.

Structure Calculations. The NMR solution structure was calculated using the program CNS using NOEs and proton chemical shifts as constraints (*18*). Only residues 4−63 (corresponding to residues 489−548 in the protein) were included in the structure calculations. NOE distance constraints were grouped into three categories: strong (1.8−2.7 Å), medium (1.8−3.3 Å), and weak (1.8−4.3 Å). Appropriate pseudoatom corrections were added to the upper limits involving methyl, aromatic, or unresolved methylene groups.

Structure calculations were performed using the torsion angle dynamics (*19*) and simulated annealing protocol incorporated into CNS. Initial structures included distance constraints between the three cysteinate sulfur atoms and the zinc (S−Zn distance of 2.30 Å). Upon identification of the metal-binding His, a distance constraint was added between the ϵ-nitrogen of His38 and the zinc (N−Zn distance of 2.0 Å). In the final rounds of refinement, the metal-binding ligands were constrained into a tetrahedral conformation with S−S distances of 3.76 ± 0.2 Å, S−N distances of 3.52 ± 0.2 Å, Zn−$N_{\epsilon 2}$−$C_{\delta 2}$/$C_{\epsilon 1}$ angles of 126°, and Zn−S_γ−C_β angles of 109.5°. The structure was refined using proton chemical shift values but no torsional angles as constraints.

Cobalt(II) Binding Studies. Cobalt(II) binding was monitored in 100 mM HEPES buffer (pH 6.9) containing 50 mM NaCl. Absorption spectra were measured on a Perkin-Elmer Lambda 9 spectrophotometer.

RESULTS

The one-dimensional NMR spectra of both the NZF-1(487−584) and NZF-1(487−548) constructs showed chemical shift changes upon the addition of zinc (data not shown). We initially pursued the solution structure of protein fragment NZF-1(487−584), a 99-amino acid fragment that includes two zinc-binding domains (*8*). The two zinc-binding domains are 68% identical in sequence over the 25-amino acid metal-binding domain core, suggesting that the two domains have very similar three-dimensional structures and would have similar stabilities. Multidimensional NMR experiments, however, revealed that many of the resonances from protons in the second domain were relatively broad and difficult to assign unambiguously compared to those from the first domain. Furthermore, the resonances from the second domain overlapped those from the first domain, complicating spectral analysis. Therefore, we continued our studies with fragment NZF-1(487−548), a 63-amino acid fragment lacking the

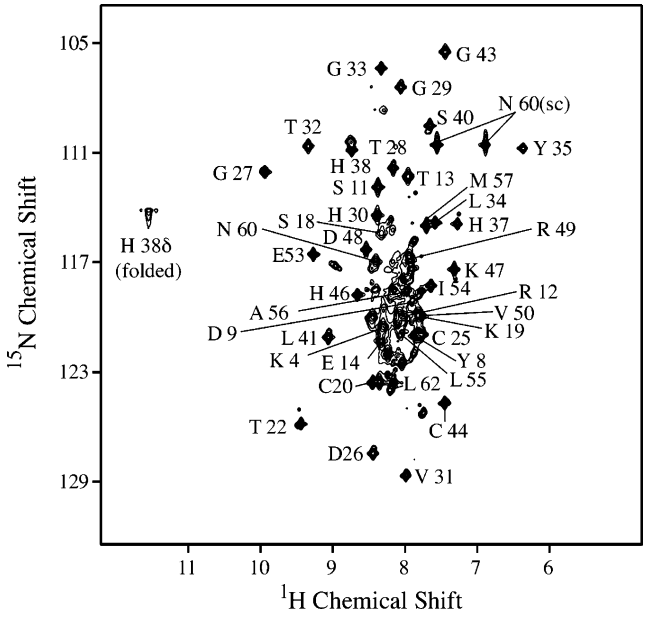

FIGURE 1: ^{1}H−^{15}N HSQC spectrum of NZF-1(487−548) at 30 °C with assigned resonances labeled. Residues that were not assigned include M1, H2, V3, K5, T6, Y7, P10, K15, R16, E17, P21, P23, G24, P36, R39, S42, P45, P51, P52, H58, E59, V61, and K63.

second domain. NMR studies, in particular the ^{1}H−^{15}N HSQC experiment, revealed that nearly all of the resonances corresponding to the first domain, including the linker, have essentially the same positions as those of the two-domain fragment NZF-1(487−584). Initial ^{1}H, ^{15}N, and ^{13}C assignments were made using ^{15}N-labeled and ^{15}N- and ^{13}C-labeled samples of NZF-1(487−584). Further experiments were carried out with ^{1}H- and ^{15}N-labeled NZF-1(487−548), and the solution structure of this fragment was determined. Nearly complete ^{1}H and ^{15}N backbone resonance assignments were obtained for residues 17−57 using standard triple-resonance assignment strategies. Ring systems for Tyr35 (^{1}H), His30, His37, His38, and His46 (^{1}H and ^{15}N) were also fully assigned. Figure 1 shows the assigned ^{1}H−^{15}N HSQC spectrum.

Analysis of Histidine Residues. Several experiments were performed to characterize the His ring systems. A ^{1}H−^{13}C CT-HSQC spectrum (*13*) allowed the identification of the carbon-bound hydrogens. On the basis of the ^{13}C chemical shift values for the NZF-1(487−584) peptide, all identifiable His residues were primarily in the $N_{\epsilon 2}$-H tautomeric form ($C_{\delta 2}$ chemical shifts of <121 ppm) with the exception of one found in the $N_{\delta 1}$-H form ($C_{\delta 2}$ chemical shift of 126.8 ppm). For both NZF-1 constructs, the ring $H_{\delta 2}$ resonances were assigned for His30, His37, His38, and His46 by means of a ^{1}H−^{15}N HSQC-NOESY (*17*) experiment. Ring system assignments for these residues were completed using a 2D ^{1}H−^{15}N HSQC (*14*) spectrum optimized for spin−spin coupling of the ring nitrogens. On the basis of this analysis, we determined that His38 is in the $N_{\delta 1}$-H tautomeric form. Furthermore, a proton resonance observed at 11.55 ppm is part of this spin system and was identified as being due to His38 $H_{\delta 1}$. The protonation state of this His residue is consistent with its role in binding the metal ion through its N_{ϵ} atom.

To obtain further evidence which shows His is directly bound to the metal ion, we replaced zinc with ^{113}Cd in NZF-1(487−548). Substitution of cadmium for zinc has been shown to preserve the structure and DNA binding activities for some zinc-binding domains. ^{113}Cd is NMR active, and heteronuclear spin−spin coupling may be observed for atoms directly bound to the metal. We collected a long-range 2D

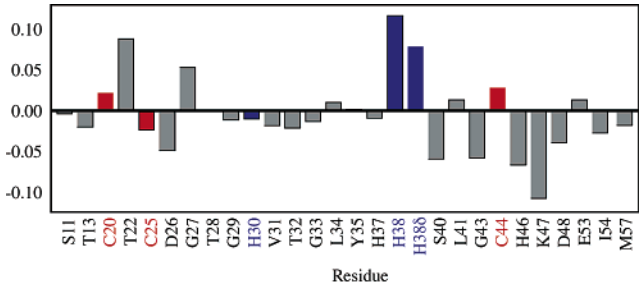

FIGURE 2: Differences in the proton chemical shifts for peptide amides between Zn(II)- and Cd(II)-substituted NZF-1(487−548). Note that the largest changes are observed near the Cys residues (shown in red) and His38 (shown in blue). Very small changes are observed adjacent to His30 (blue). The chemical shift of the His38 δ resonance is also shown. Residues were not included where the chemical shifts for either the Zn(II) or Cd(II) complex could not be uniquely determined.

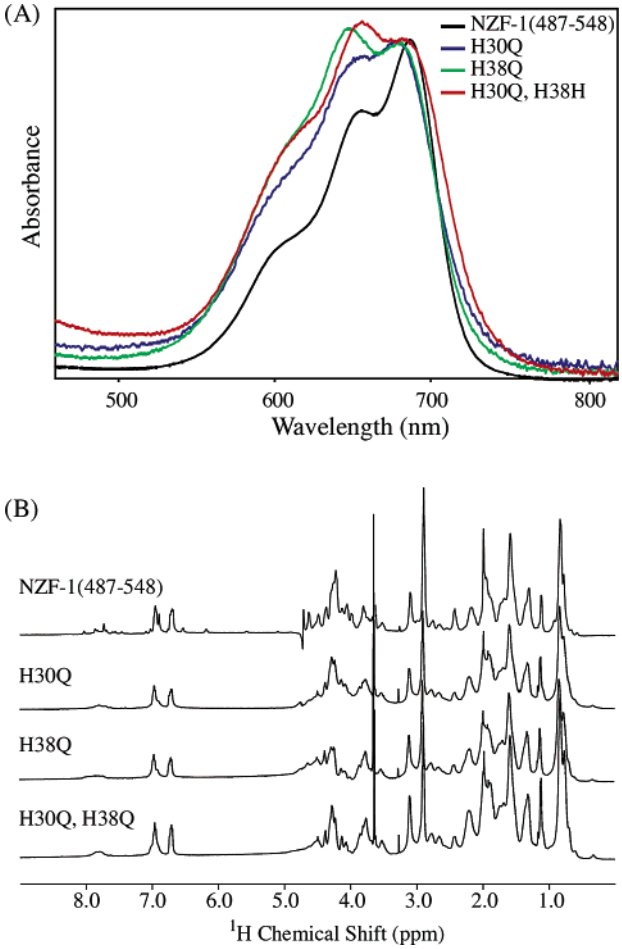

FIGURE 3: (A) Comparison of the absorption spectra in the visible region of the cobalt(II) complexes of NZF-1(487−548) and mutants with one or both of the conserved His residues converted to Gln. The spectra of all of the mutants differ somewhat from that of the wild type, but all are consistent with Cys_3His-Co chromophores. (B) Comparison of the ^{1}H NMR spectra in D_2O of the zinc(II) complexes of NZF-1(487−548) and the His to Gln mutants. Only the wild-type fragment shows evidence of a well-defined structure as revealed particularly by the dispersion in the aromatic region (6−8 ppm). Experiments were performed at 20 °C.

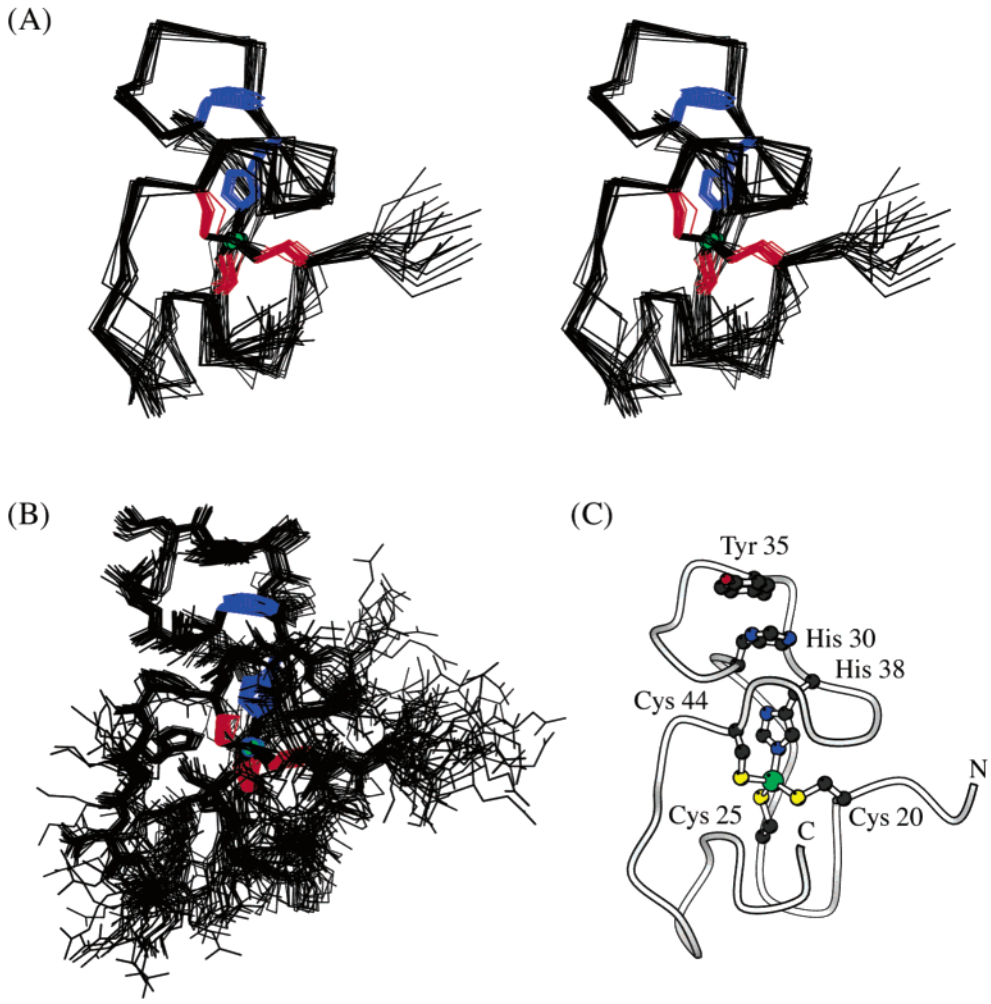

FIGURE 4: (A) Stereoview of the aligned backbones of 20 structures, including residues 17−57 from NZF-1(487−548). The side chains of the Cys residues (red) and the conserved His residues (blue) are also shown. (B) Twenty aligned structures showing all non-hydrogen atoms. (C) Schematic view in the same orientation with the Cys residues, conserved His residues, and Tyr35 labeled. Note that the side chain of His30 lies between metal-bound His38 and Tyr35.

$^{1}H-^{15}N$ HSQC spectrum for the ^{113}Cd-substituted protein with the goal of observing splitting of the signals due to the cadmium-bound nitrogen atom (*20*). However, the nitrogen signals in this spectrum were too broad to observe clear splittings. We also collected a $^{1}H-^{15}N$ HSQC spectrum optimized for short-range correlation between amide nitrogens and hydrogens. The HSQC spectra for the Cd(II)-bound and Zn(II)-bound forms were quite similar overall. Small chemical shift changes were observed for some resonances, presumably due to small structural changes associated with the differences in ion radius between Cd(II) (0.97 Å) and Zn(II) (0.74 Å). Significantly, the resonances for all three cadmium-bound cysteines and for His38 were shifted, while those for His30 were unaltered (Figure 2). This result provides further evidence that His38 is directly metal-bound whereas His30 lies further from the metal center.

We attempted to confirm this result by mutational analysis. His30 and His38 were individually substituted with glutamine, and the metal binding properties of the mutated proteins were examined by titration with cobalt(II). Consistent with results from studies with synthetic peptides corresponding to a different domain of NZF-1 (*9*), the absorption spectra of the cobalt(II) complexes of both of these mutated fragments were only slightly different from those of the wild-type fragment (Figure 3A). This suggests a level of flexibility within the polypeptide that allows other His residues to move in to coordinate metal in the absence of the normal metal-binding ligand. This flexibility is further underscored by characterization of a double mutant in which both His30 and His38 are mutated to glutamine. Mutation of both conserved His residues in a peptide corresponding to a different domain from NZF-1 resulted in dramatic changes in the cobalt binding properties (*9*). In contrast to this result, the absorption spectrum of the cobalt(II) complex of doubly mutated NZF-1(487−548), H30Q/H38Q, was very similar to those of the other mutants. This suggests that yet another His residue can bind the cobalt(II) ion when the two conserved His residues are absent; His37 is a likely candidate. The folded states of the zinc(II) complexes of the mutated fragments were examined by one-dimensional ^{1}H NMR (Figure 3B). The spectra all showed substantial differences from that of the wild type and displayed spectral features indicating that the mutated fragments were folded substantially less well than the wild-type fragment. Thus, both conserved His residues appear to be essential for a stably folded structure.

Structure Determination. A total of 372 NOE distance restraints were used in the NZF-1(487−548) structure calculations. The majority of these NOEs are found within the zinc-binding core and 12 residues extending past the final metal-binding Cys residue. The N-termini (residues 1−16)

Table 1: Structural Statistics for NZF-1(487−548)

rmsd from average structure (Å)	
backbone[a]	1.04 ± 0.19
all heavy atoms[a]	1.94 ± 0.25
rmsd from experimental distance restraints (Å)	0.046 ± 0.003
rmsd from proton chemical shifts	
all	0.43 ± 0.01
Hα	0.36 ± 0.02
Hβ	0.36 ± 0.02
HN	0.61 ± 0.03
deviations from the idealized covalent geometry	
bonds (Å)	0.0042 ± 0.0002
angles (deg)	0.59 ± 0.03
impropers (deg)	0.42 ± 0.03
PROCHECK	
no. of distance restraints	
all	372
intraresidue	153
sequential	77
medium-range ($1 < \|i - j\| \leq 4$)	56
long-range ($\|i - j\| > 4$)	86
percentage of residues with ϕ and ψ	
in most favored regions	34.2
in additionally allowed regions	38.9
in generously allowed regions	14.6
in disallowed regions	12.3

[a] Statistics are presented for 20 structures for residues 17−57.

and C-termini (residues 58−63) are poorly determined and are not included in the structures presented. A total of 20 final structures were generated from random initial coordinates by simulated annealing. The average rmsd value relative to the mean coordinates for residues 17−57 is 1.04 Å for the backbone atoms and 1.94 Å for all heavy atoms. These values drop to 0.55 and 1.28 Å, respectively, when only residues 20−44 are considered. The superposition of residues 17−57 for the 20 structures is depicted in Figure 4. The loop regions between the zinc-binding ligands are better defined with backbone rmsd values of 0.44 Å for residues 20−25, 0.27 Å for residues 25−38, and 0.50 Å for residues 38−44 even though assignments for P23, G24, R39, and S42 were not obtained. The family of structures was analyzed using the program PROCHECK-NMR (*21*). A summary of statistics associated with the structure calculations is provided in Table 1. The coordinates for NZF-1(487−548) have been deposited in the Protein Data Bank and the Biomagnetic Resonance Bank.

DISCUSSION

The structure of the NZF-1 metal-binding domain is distinct from those of all previously characterized metal-binding domains and, indeed, all other structures based on a search of the DALI database (*22*). The determined structure reveals the roles of the two conserved His residues (Figure 4C). The second of the two His residues (His38) is bound to the metal ion through its ϵ-nitrogen. The ϵ-nitrogen more commonly coordinates zinc ions in other zinc-binding domains that feature histidine coordination. This His side chain is buried within the core of the structure, contacting backbone atoms of residues Gly27, Ser40, Cys44, and Pro45 as well as the side chain of His30. The buried nature of this residue presumably is responsible for the clearly observable resonances for the proton bound to the δ-nitrogen of this residue. His30 lies adjacent to the side chain of His38. In addition, His30 stacks against the side chain of Tyr35. Examination of the sequences of members of this domain family reveals that the residue in position 35 is Tyr or Phe in more than 75% of the sequences. In almost all of the remaining sequences, the residue in this position is Arg. Indeed, the second domain in NZF-1(487−584) has Arg in this position. The lack of an aromatic residue in this position suggests a possible explanation for why the second domain in NZF-1(487−584) is less dynamically stable than the first.

The metal-binding domain has the form Cys-X_4-Cys-X_{12}-His-X_5-Cys. This is similar in spacing to the TFIIIA-like zinc-binding domain (Cys-X_{2-4}-Cys-X_{12}-His-X_{3-5}-His) (*1*, *23*, *24*). Yet the structures of each of the three metal-chelating loops are quite different in these two domain families. The first loop has the form Cys-X_4-Cys. In the NZF-1 family, the sequence of this loop is highly conserved with the consensus sequence Cys-Pro-Thr-Pro-Gly-Cys. The two conserved Pro residues enforce a relatively extended conformation for this loop. This precludes the formation of the more compact TFIIIA-like Cys-X_4-Cys loop. The second loop has the form Cys-X_{12}-His and has a relatively extended structure. This loop is collapsed with few side chains on the interior of the loop. Tyr35 and His38 are stacked together on the outside of this loop. This stands in contrast to the Cys-X_{12}-His loop from TFIIIA-like domains that have similar overall dimensions but have an interior hydrophobic core, including the conserved Phe and Leu residues, characteristic of these domains. The final loop in the NZF-1 structure differs from that in TFIIIA-like domains in that it is less regular than the helical structure found in TFIIIA-like domains and it terminates with a Cys residue rather than a His.

This final loop is followed by a region of approximately 12 residues that is reasonably well ordered in solution. This region extends away from the structure for approximately four residues, turns, and then forms a short stretch of helix-like structure. This region appears to be stabilized by at least two interactions. First, the NH group of His46 forms a

hydrogen bonding interaction with the cysteinate sulfur atom of Cys44. Second, the side chain of Ile54 participates in a hydrophobic core that includes Leu41 and the methylene group of Cys44.

Ideally, determination of this structure would suggest how these domains interact with DNA. Unfortunately, the observed structure lacks regular secondary structural elements such as α-helices that are frequently involved in sequence-specific interactions with DNA. However, three properties of the members of the NZF-1 family suggest constraints for a complex with DNA. First, as noted above, NZF-1 binds in the major groove based on methylation interference studies (*5*). Second, the binding sites for members of the NZF-1 family tend to have approximate 2-fold symmetry (*7*). This suggests that the protein unit that binds to this site would also have approximate 2-fold symmetry. Previous studies have revealed that two NZF-1 domains are required for high-affinity DNA binding (*5*). Models in which two domains, related by an approximate 2-fold symmetry axis, bind together to a single site are consistent with these observations. Third, the amino and carboxyl termini of the domain enter and exit the structure from the same direction, suggesting that the domain that precedes the metal-binding unit and the linker region that connects the two metal-binding units lie on one face of the structure. Given the variability of these non-metal-binding domain regions, this face must lie away from the DNA to avoid unfavorable steric interactions. Computer-based models consistent with all of these constraints have been constructed on the basis of the structure of the domain that we have determined, revealing that these constraints can be satisfied simultaneously. However, further information is required to define the structure of the complex more fully.

CONCLUSION

The determination of the structure of this fragment of NZF-1 reveals a novel fold for its zinc-binding domain. This structure provides at least a partial explanation for the conservation of two His residues within this sequence family. Analysis of this structure and other observations suggests that each of these domains interacts with a half-site within a pseudosymmetric DNA binding site. The structure of the domain provides a framework for the selection of site-directed mutants in identifying residues that play specific roles in DNA binding and for the design of future structure studies that will reveal the DNA binding mode of these domains.

REFERENCES

1. Berg, J. M. (1986) *Science 232*, 485−487.
2. Pabo, C. O., and Sauer, R. T. (1992) *Annu. Rev. Biochem. 61*, 1053−1095.
3. Berg, J. M., and Shi, Y. (1996) *Science 271*, 1081−1085.
4. Kim, J. G., and Hudson, L. D. (1992) *Mol. Cell. Biol. 12*, 5632−5639.
5. Jiang, Y., Yu, V. C., Buchholz, F., O'Connell, S., Rhodes, S. J., Candeloro, C., Xia, Y. R., Lusis, A. J., and Rosenfeld, M. G. (1996) *J. Biol. Chem. 271*, 10723−10730.
6. Bellefroid, E. J., Bourguignon, C., Hollemann, T., Ma, Q., Anderson, D. J., Kintner, C., and Pieler, T. (1996) *Cell 87*, 1191−1202.
7. Yee, K. S., and Yu, V. C. (1998) *J. Biol. Chem. 273*, 5366−5374.
8. Berkovits, H. J., and Berg, J. M. (1999) *Biochemistry 38*, 16826−16830.
9. Blasie, C. A., and Berg, J. M. (2000) *Inorg. Chem. 39*, 348−351.
10. Cai, M., Huang, Y., Sakaguchi, K., Clore, G. M., Gronenborn, A. M., and Craigie, R. (1998) *J. Biomol. NMR 11*, 97−102.
11. Marion, D., Driscoll, P. C., Kay, L. E., Wingfield, P. T., Bax, A., Gronenborn, A. M., and Clore, G. M. (1989) *Biochemistry 28*, 6150−6156.
12. Kay, L. E., Xu, G.-Y., Singer, A. U., Muhandirum, D. R., and Forman-Kay, J. D. (1993) *J. Magn. Reson., Ser. B 101*, 333−337.
13. Shimba, N., Takahashi, H., Sakakura, M., Fujii, I., and Shimada, I. (1998) *J. Am. Chem. Soc. 120*, 10988−10989.
14. Pelton, J. G., Torchia, D. A., Meadow, N. D., and Roseman, S. (1993) *Protein Sci. 2*, 543−558.
15. Farmer, B. T., Venters, R. A., Spicer, L. D., Wittekind, M. G., and Mueller, L. (1992) *J. Biomol. NMR 2*, 195−202.
16. Wittekind, M., and Mueller, L. (1993) *J. Magn. Reson., Ser. B 101*, 201−205.
17. Mori, S., Abeygunawardana, C., van Zijl, P. C., and Berg, J. M. (1996) *J. Magn. Reson., Ser. B 110*, 96−101.
18. Brunger, A. T., Adams, P. D., Clore, G. M., DeLano, W. L., Gros, P., Grosse-Kunstleve, R. W., Jiang, J. S., Kuszewski, J., Nilges, M., Pannu, N. S., Read, R. J., Rice, L. M., Simonson, T., and Warren, G. L. (1998) *Acta Crystallogr. D54* (Part 5), 905−921.
19. Stein, E. G., Rice, L. M., and Brunger, A. T. (1997) *J. Magn. Reson., Ser. B 124*, 154−164.
20. Damblon, C., Prosperi, C., Lian, L.-Y., Barsukov, I., Soto, R. P., Galleni, M., Frere, J. M., and Roberts, G. C. K. (1999) *J. Am. Chem. Soc. 121*, 11575−11576.
21. Laskowski, R. A., Rullmannn, J. A., MacArthur, M. W., Kaptein, R., and Thornton, J. M. (1996) *J. Biomol. NMR 8*, 477−486.
22. Holm, L., and Sander, C. (1993) *J. Mol. Biol. 233*, 123−138.
23. Berg, J. M. (1988) *Proc. Natl. Acad. Sci. U.S.A. 85*, 99−102.
24. Lee, M. S., Gippert, G. P., Soman, K. V., Case, D. A., and Wright, P. E. (1989) *Science 245*, 635−637.

BI035159D